Recent changes in the ECMWF NWP system

Mohamed Dahoui, Niels Bormann, Stephen English, Reima Eresmaa, Alan Geer, Heather Lawrence, Peter Lean, Katrin Lonitz, Cristina Lupu, Tony McNally and Peter Weston

ECMWF, Shinfield Park, Reading, UK

mohamed.dahoui@ecmwf.int

Changes since ITSC-20

New model cycles

Since ITSC-20, ECMWF implemented three substantial upgrades of its Integrated Forecasting System (IFS). The three upgrades (**41R2**, **43R1** and **43R3**) had a significant positive impact on forecast skill in the medium range and monthly forecasts.

Resolution increase:

- New cubic octahedral grid
- The High resolution system upgraded to higher resolution Tco1279 ~9km (**41R2**)
- The Ensembles upgraded to a higher resolution Tco639 ~16km (days 1-15) and Tco319 ~32km (days 16-46) (**41R2**)
- Increased horizontal resolutions for the HRES 4DVAR and EDA (**41R2**)
- The Ocean model (NEMO) resolution increased to 0.25°and 75 levels (**43R1**)

Observations:

- Activation of F-18 humidity sounding channels over ocean and extend all-sky assimilation to snowy land surfaces (**41R2**)
- Situation dependent observation errors for AMSUA (**41R2**)
- Improved IASI aerosol screening (**41R2**)
- 25% increase of GPSRO observation errors (**41R2**)
- Update of RTTOV coefficient files for microwave instruments (**41R2**)
- Allow Meteosat mid-height IR AMVs (**41R2**)
- Assimilation of aircraft humidity (**41R2**)
- Viewing geometry (slantwise path) fully taken into account when simulating radiances from clear-sky sounders (**43R1**) – See presentation 2.03 by N. Bormann
- Update observation error covariance for IASI and CrIS (**43R1**)
- New channel selection for CrIS (118 channels instead of 78) (**43R1**). See poster 9p.01 by R. Eresmaa
- Update of aerosol detection scheme for IASI, AIRS and CrIS to be independent from bias correction (**43R1**)
- Assimilation of snowfall from the NEXRAD RADAR network over the USA (**43R1**)
- Activation of new microwave humidity sounders: SAPHIR and GMI (**43R3**)
- Activation of 118 GHz channels over land from MWHS-2 instrument on-board FY-3C (**43R3**) – See poster 3p.04 by H. Lawrence
- Harmonised data usage over land and sea-ice for microwave sounders (**43R3**) – See poster 10p.04 by N. Bormann
- Improved quality control for radio occultation observations and radiosonde data (**43R3**)
- Improved screening of infrared observations for anomalously high atmospheric concentrations of hydrogen cyanide (HCN) from wildfires (**43R3**)

Data assimilation changes:

- EDA cycling its own background errors (**41R2**)
- Compute scale-dependent hybrid background error covariance (B) by adding samples from latest EDA forecast to static climatological B with increasing weight of today's EDA for smaller wavelengths (**41R2**)
- Improved calculation of humidity saturation for very cold temperatures (**41R2**)
- Upgrade of SST perturbations used in the EDA (**43R1**)
- Reactivation in the stratosphere of weak constraint option in the 4DVAR (**43R1**)
- New Ocean analysis/reanalysis (ORAS5) (**43R1**)
- Improved assimilation of screen level SYNOP observations in the land surface analysis (**43R1**)
- Improved EDA derived background estimates used in the 4DVAR (**43R1**)
- Improved humidity background error variances directly from the EDA (**43R3**)
- Revised wavelet filtering of background error variances and revised quality control of dropsonde wind observations in 4DVAR to improve tropical cyclone structures (**43R3**)

Model changes:

- Improved representation of radiation-surface interaction (**41R2**)
- Improved freezing rain physics (**41R2**)
- Improved parcel perturbation for deep convection (**41R2**)
- Inclusion of surface-tiling for long-wave radiation interactions (**41R2**)
- Improved solar zenith angle calculation (**41R2**)
- Improvements of linear physics used in the data assimilation for gravity wave drag (**41R2**)
- Usage of new CAMS ozone climatology (**43R1**)
- Changes to boundary layer cloud for marine stratocumulus and at high latitudes (**43R1**)
- Modifications to surface coupling for 2 metre temperature (**43R1**)
- New, more efficient and improved radiation scheme (**43R3**)
- New aerosol climatology based on 'tuned' CAMS aerosol re-analysis including dependence on relative humidity (**43R3**)
- Increased super-cooled liquid water at colder temperatures (down to -38C) from the convection scheme (**43R3**)

Timeline of operational changes applied to radiances

SON 2015
- Blacklist of NOAA-18/AMSUA Ch5 and Ch8
- Blacklist of IASI/CrIS/AIRS HCN channels
- Increased noise of Metop-A/HIRS

DJF 2016
- Activation of MET-10/CSR and HIMAWARI-8 CSR
- Activation of Metop-A/HIRS
- Blacklist of MET-10/CSR and Metop-A/HIRS
- Blacklist of MTSAT-2/CSR

MAM 2016
- Activation FY-3C/MWHS2
- Blacklist Metop-A/HIRS
- Drift of IR window ch bias due to OSTIA-SST
- Blacklist NOAA-18/MHS

JJA 2016
- Re-activation NOAA-18/MHS

SON 2016
- Re-activation F17/SSMIS
- Re-activation Metop-B/AMSUA stratospheric channels
- AQUA/AMSUA outage
- Blacklist F17/SSMIS (183 GHz channels)
- Blacklist Metop-B/AMSUA (Ch5-8)
- Blacklist FY-3B/MWHS

DJF 2017
- Re-activation Metop-B/AMSUA Ch 5-8, Metop-A/MHS and FY-3B/MWHS
- Re-activation AQUA/AMSUA and FY-3B/MWHS
- Blacklist Metop-A/MHS
- Blacklist FY-3B/MWHS

MAM 2017
- MET-8 CSR over Indian Ocean
- Re-activation ATMS
- Blacklist MET-7 CSR
- Blacklist ATMS (calibration upgrade)
- Outage FY-3C/IRAS (~ one month)
- Cessation EARS NOAA-15 AMSUA
- Blacklist Metop-A/AMSUA Ch5

JJA 2017
- Re-activation Metop-A/AMSUA Ch5
- Activation SAPHIR and GMI (43R3)
- Non-linearity correction Metop-B/IASI
- AIRS outage (4 days)

SON 2017
- Re-activation NOAA-19/MHS and NOAA-18/AMSUA Ch5 and 8
- NOAA-19/MHS anomaly

Microwave sounders/imagers usage

	AMSUA	MHS (all sky)	ATMS	SSMIS (all sky)	MWHS	MWHS2 (all-sky)	SAPHIR (all-sky)	GMI (all-sky)	AMSR2 (all-sky)
Metop-A	5,6,9-14	3-5							
Metop-B	5-14	3-5							
NOAA-15	5,7-10,12-13								
NOAA-18	5-8,10-14	3-5							
NOAA-19	5-6,9-14	4-5							
AQUA	8-14								
NPP			6-15,18-22						
F-17				9-11,12-14,16-17					
F-18				9-11					
FY-3B					3-5				
FY-3C						2-7,11-12,15			
Megha-Tropiques							1-5		
GCOM-W1									7-11,13
GPM								3-6,8,12-13	

Table 1: Assimilated microwave sounding/imaging channels

Recent changes:

- Addition of all-sky 183 GHz observations from GMI and SAPHIR. Even on top of 9 other 183 GHz microwave sounders, these instruments still gave positive benefits (see Figure 1) suggesting that the impact of all-sky humidity sounding data has not yet saturated.

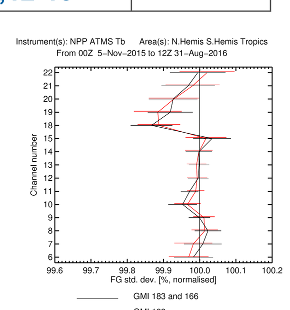

Figure 1: impact of assimilating GMI 183 GHz channels, as measured by the normalised change in std. dev. of FG departures against ATMS. Note that "183 + 166" tests also the assimilation of 166 Ghz channels, which was not adopted operationally but will be tested in a future cycle

Hyper-spectral infrared sounders usage

	Long-wave	Window + Ozone	Water Vapour	Short-wave
Metop-A IASI	153	28	9	1
Metop-B IASI	153	28	9	1
AIRS	81	32	7	19
CrIS	88	23	7	

Table 2: Number of channels used

Recent changes:

- Updated list of CrIS channels (118 channels instead of 78)
- Updated observation error covariance matrices (with inter-channel error correlations) for IASI and CrIS
- New aerosol detection scheme
- Update ozone anchor channels for IASI and CrIS

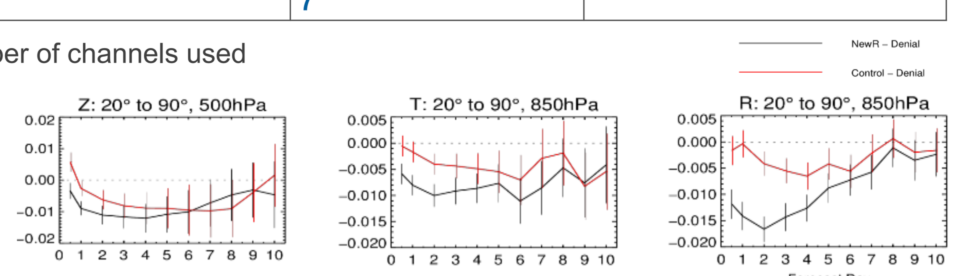

Figure 2: Forecast impact on Geopotential height of the new IASI observation error covariance matrix (normalised difference in RMSE vs own analysis)

Geostationary radiances usage

	SEVIRI	GOES Imager	AHI
METEOSAT-10	6.2 and 7.3 micron (WV)		
METEOSAT-8	6.2 and 7.3 micron (WV		
GOES-13		6.7 micron (WV)	
GOES-15		6.7 micron (WV)	
HIMAWARI-8			6.2, 6.9 and 7.3 micron (WV)

Table 3: Assimilated geostationary radiances

Slant-path radiative transfer for sounder radiances

- Slanted satellite geometry fully taken into account in the simulation and assimilation of clear sky radiances from sounders.
- Significant improvements in the simulation of brightness temperatures from model fields. This is most noticeable for large zenith angles for upper tropospheric and stratospheric channels.
- Slant-path RT leads to better agreement with observations
- Overall positive impact especially in the on the stratospheric and at short ranges

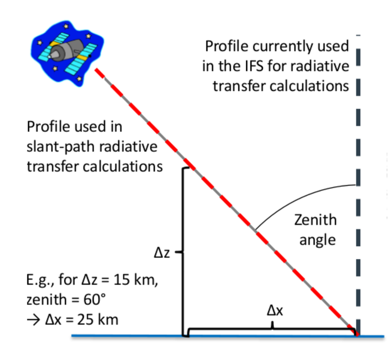

Figure 3: Schematic of satellite viewing geometry. The red path is used in slant-path calculations

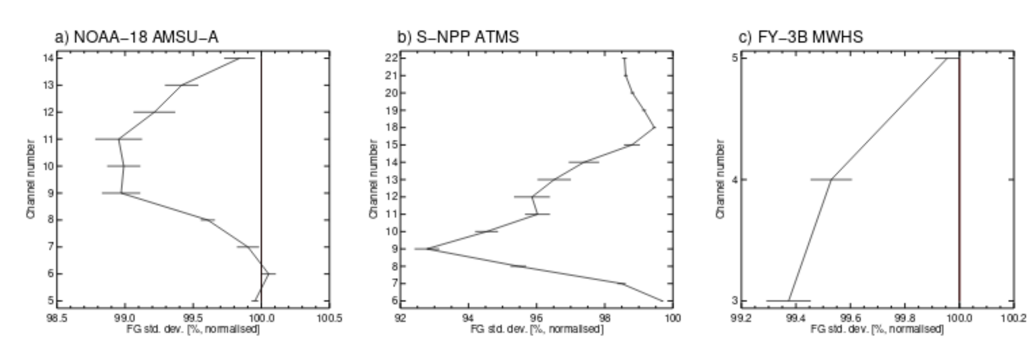

Figure 4: Standard deviation of differences between observations and simulations that take the slant-path geometry into account, normalised by equivalent values obtained with simulations that ignore the slant-path geometry. Values below 100 % indicate smaller standard deviations when the slant-path geometry is taken into account. Statistics are for NOAA-18 AMSUA, S-NPP ATMS and FY-3B MWGS

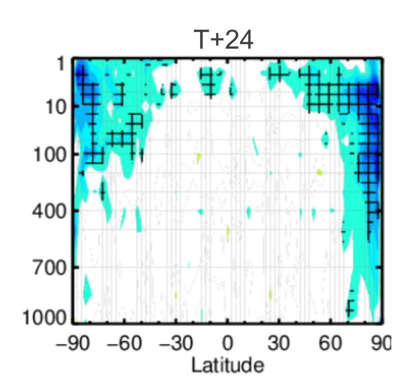

Figure 5: Normalised differences in standard deviation of vector wind analysis increments (for T+24) between slant-path experiment and the control

Main upcoming satellite changes (cycle 45R1)

The upcoming ECMWF model cycle 45R1 (expected to be implemented in Q1 2018) will include significant various data assimilation changes:

- Improved radiative transfer model RTTOV-12 (see poster 1p.05 by C. Lupu)
- Improved treatment of biases (Constrained VarBC) for AMSUA channel 14 and ATMS channel 15 (see presentation 12.02 by W. Han)
- Infrared radiances over land (see presentation 10.01 by R. Eresmaa)
- Improved usage of all sky radiances in coastal areas
- Use of DBNet MWHS2

Acknowledgments

ECMWF gratefully acknowledge the invaluable funding from EUMETSAT and ESA and collaboration with other agencies, notably CMA, JMA, NOAA and NASA. Thanks to Anabel Bowen and Simon Witter for the help with the poster.